Polym. Bull. (2011) 66:211–222
DOI 10.1007/s00289-010-0323-9

ORIGINAL PAPER

Degradation and stabilization of poly(3-hexylthiophene) thin films for photovoltaic applications

Gianmarco Griffini · Stefano Turri · Marinella Levi

Received: 25 March 2010 / Revised: 3 June 2010 / Accepted: 10 June 2010 /
Published online: 17 June 2010

Abstract Polymer-based solar cells (PSC) represent a promising technology in the field of photovoltaics, although they still suffer from poor environmental stability. Poly(3-hexylthiophene) (P3HT) is one of the most commonly employed electron-donor materials for the preparation of the photo-active layer of PSC and it is known to undergo degradation when exposed to light. In this work, the degradation of P3HT was studied by irradiating polymer films by means of simulated sunlight. The results of this study highlighted a remarkable instability of P3HT. Substantial modifications of the infrared as well as of the UV–Vis spectra of the polymer were reported and a degradation pathway was suggested, in agreement with recent literature results. In order to stabilize the structure, two additives were evaluated namely a standard Hindered Amine Light Stabilizer (HALS) and Multi-Walled Carbon Nanotubes (MWCNT). The addition of MWCNT appeared to significantly reduce the rate of degradation.

Keywords Poly(3-hexylthiophene) · Photovoltaic · Degradation · Stabilization · Multiwall carbon nanotube

Introduction

Polymer-based solar cells (PSC) represent nowadays a possible alternative to more traditional silicon-based photovoltaic technology [1]. Indeed, the light weight of the materials used as well as the opportunity of employing flexible substrates for their fabrication open up the possibility for new applications such as large-area non-planar devices. However, PSC still show limited power conversion efficiencies and

G. Griffini · S. Turri (✉) · M. Levi
Dipartimento di Chimica, Materiali e Ingegneria Chimica "Giulio Natta", Politecnico di Milano, Piazza Leonardo da Vinci 32, 20133 Milan, Italy
e-mail: stefano.turri@polimi.it

suffer of relatively poor environmental stability which limits their operational lifetime compared to inorganic-based photovoltaic technology [2].

Although environmental stability of PSC still represents a challenge towards PSC deployment on industrial scale, significant progresses in terms of manufacture and demonstration have been recently made. In particular roll-to-roll manufacturing processes based on all printing techniques have been employed to fabricate devices on flexible substrates with inverted cell geometry [3, 4] and with ITO-free fabrication steps [5, 6]. In addition, the relative stability towards degradation of encapsulated large area PCS has been demonstrated through round robin and inter-laboratory studies on devices fabricated on flexible substrates using full roll-to-roll processing techniques [7]. Recently, field studies involving the fabrication of flexible PSC modules in ambient conditions through full roll-to-roll processes have also been presented [8] and the integration of PSC modules into commercial products has been shown [9].

In the most efficient PSC prototypes [10], the photoactive layer is typically made of a blend of an electron-acceptor and an electron-donor material, where the latter is constituted by a semiconducting conjugated polymer. Among the most commonly employed electron-donor materials, poly(3-hexylthiophene) (P3HT) is receiving a great deal of attention, due to its good electrical and mechanical properties as well as its ability to be easily processed in solution of common organic solvents [11]. Furthermore, P3HT appears to be more environmentally stable than other semiconducting conjugated polymers, but also devices based on this material are susceptible to chemical degradation. In particular, the interaction of oxygen, water and light with the materials constituting the active polymer layer and the metallic electrode leads to a decay of the photovoltaic performances over time [12, 13]. Nevertheless, the fabrication of air stable PSC has been reported on an inverted device geometry where the active layer is constituted by a bulk heterojunction of zinc oxide nanoparticles and poly-(3-carboxydithiophene) (P3CT) [14].

In addition to the stability in the complete PSC devices, the photo-degradation of the active conjugated polymer still represents a challenge. Indeed, P3HT stability towards light still appears to be poor and the mechanisms underlying its degradation have to be fully clarified, especially in the solid state.

One of the first studies on the stability of P3HT towards light was carried out by Abdou and Holdcroft [15]. In their work, P3HT in chloroform solution containing dissolved molecular oxygen was irradiated by UV and visible light. Degradation of the polymer was observed and two degradation pathways were proposed. The first involved the photosensitized formation of singlet oxygen $O_2(^1\Delta_g)$ by the triplet state of P3HT causing formation of endoperoxide species which would lead in turn to reduction of π-conjugation and polymer photobleaching. The second involved free-radical attack of photosensitized trace amounts of transition-metal salts to the lateral alkyl chain leading to chain scission and formation of carbonyl and hydroxyl adducts as well as crosslinking. Based on these observations, in a later work by the same group [16] a mechanism accounting for the solid state behaviour of P3HT was subsequently proposed. However, no suggestions were given on possible ways to decrease the degradation rate.

A similar free-radical mechanism was suggested for the thermo-oxidative degradation of poly(3-octylthiophene) (P3OT) in the solid state [17] with formation of a ketonic group in the α-carbon position of the alkyl side chain of the polymer. The effect of stabilizers on the degradation of P3OT was also studied, by employing different classes of stabilizers, namely primary antioxidants, secondary antioxidants, antioxidants reacting with nonoxygenated radicals, metal deactivators, and light stabilizers in the form of radical scavengers. However, no clear positive effects on the degradation rate of P3OT were observed by FTIR and SEC analyses. This was attributed to the high sensitivity of hydrogen abstraction from the α-carbon position of P3OT which could lead to a radical site in every alkyl group of the polymer.

In the work by Caronna et al. [18] the photodegradation of poly(3-butylthiophene) (P3BT) in the solid state was studied in different environmental conditions, namely air, nitrogen and oxygen. No degradation was observed in nitrogen atmosphere while two degradation products were isolated and identified after irradiation in air. Their formation was attributed to the reaction of singlet oxygen with the polymer conjugated chain, the former generated by energy transfer from the excited state of the polymer to molecular oxygen. In addition two compounds were found to decrease the rate of polymer oxidation, namely *N*-hexadecyl-*N*-methylaniline and 1-phenyldodecan-1-one. Their stabilizing action was attributed to their ability to act as light screen thereby protecting the polymer from photo-oxidation.

The poly[2-methoxy-5-(3′,7′-dimethyloctyloxy)-1,4-phenylenevinylene] (MDMO-PPV) system in solid state was studied by Chambon et al. [19, 20] through photo- and thermal-oxidation. Infrared spectroscopy allowed to monitor the formation of ester, formate and carboxylic acid species and a degradation route was suggested involving radical oxidation of the polymer. The study was extended to the blend constituted by methano-fullerene[6,6]-phenyl C61-butyric acid methyl ester (PCBM) and MDMO-PPV. It was found that the addition of PCBM to MDMO-PPV results in a decrease of degradation rate of MDMO-PPV in blended film. This effect was attributed to radical scavenging properties of PCBM.

In a recent work by Manceau et al. [21] the accelerated photo-oxidative degradation of P3HT in the solid state was studied in the presence of air. On the basis of infrared spectroscopy results and chemical derivatization treatments, a degradation mechanism was proposed involving the radical oxidation of the hexyl side-chain and the sulphur atom of thiophene ring. Based on a previous work by the same group [22], it was also confirmed that singlet oxygen does not appear to be the main intermediate in the degradation process of P3HT. On the other hand, no suggestions were made on possible ways to decrease the degradation rate.

In the present work, a study was presented on the photo-oxidative degradation of P3HT in the solid state under simulated sunlight. A degradation mechanism was proposed confirming what reported in the literature for accelerated experiments [21]. Furthermore, the addition of two compounds to P3HT was studied, namely a Hindered Amine Light Stabilizer (HALS) and Multi-Walled Carbon Nanotubes (MWCNT), and the effect of their addition to the stabilization of P3HT was investigated.

Experimental

Poly(3-hexylthiophene) (P3HT) was purchased from Rieke Metals Inc. (type 4002, regioregularity 94%) and was used as received. Chloroform (Sigma–Aldrich) was used as solvent in all tests. Multi-walled Carbon Nanotubes (MWCNT—average diameter 9.5 nm, average length 1.5 μm, purity >95%) were purchased from NanoCyl and used as received, without any further purification. The Hindered Amine Light Stabilizer additive (TINUVIN®292) was purchased from CIBA and used as received.

Infrared spectroscopy and UV–Vis spectroscopy were performed on thin film samples (~200 nm) deposited on NaCl, KBr and glass substrates by spin coating (WS-400B-NPP, Laurell Technologies Corp.). The thickness of the samples was measured by profilometry. Infrared spectra were recorder in transmission mode on a Nicolet 760–FTIR Spectrophotometer controlled by OMNIC software. Spectra were obtained using 32 scans and a 4 cm^{-1} resolution. UV–Vis absorption spectra were recorded in transmission mode on solid state samples deposited onto glass substrates by means of a Jasco V-570 UV–Vis-NIR Spectrophotometer.

All samples were irradiated in air by means of a Class A solar simulator (Xenon short arc lamp 150 W, Abet Technologies) with AM1.5G (ASTM 927-91) spectral distribution and a power output of about 2,200 W/m^2 (approximately 2 suns). The solar simulator power output was monitored by means of a powermeter with thermopile sensor (Ophir). Samples were collected at different irradiation times.

The molecular weight of the samples was determined through Gel Permeation Chromatography (GPC—Waters 410) using THF as eluent and polystyrene standards.

^{1}H-NMR spectra were recorded on a Bruker AC 300 NMR Spectrometer. All samples for ^{1}H-NMR were dissolved in $CDCl_3$.

DSC analyses were performed on solid state samples using a DSC/823e-Mettler Toledo differential scanning calorimeter. Scan rate was 20 K/min.

Results and discussion

The molecular weights of the polymer samples were measured by gel permeation chromatography in THF. At different irradiation times the molecular weight of the polymer was determined in order to monitor modifications of the macromolecular chain length occurring after exposure to light. The pristine polymer gave values of $\bar{M}_n = 3.0 \times 10^4$ and $\bar{M}_w = 7.0 \times 10^4$, respectively. By increasing the exposure time of the cast polymer films, no significant variation of $\bar{M}_n$ and $\bar{M}_w$ was observed even after 200 h of exposure to simulated sunlight. On the other hand, a progressively higher amount of insoluble material was formed with increasing exposure time. This trend reflects the fact that the GPC analysis is limited to soluble material as it is carried-out in solution. Insoluble moieties containing degradation products, which were not found in the pristine polymer but only in degraded samples, are filtered-out before elution of the sample into the GPC and are thus excluded from the analysis.

All polymer samples were also analyzed by solution ^{1}H-NMR spectroscopy. As far as the pristine polymer is concerned, one sharp band centred at δ 6.98 was observed in the ^{1}H-NMR. This band is attributed to the thiophene proton and denotes the HT–HT regioregular structure of the polymer [23]. This regioregular structure was confirmed by the ^{1}H-NMR spectrum in the α- and β-methylene proton region, where only the signals corresponding to HT linkage were present (Fig. 1a).

As far as the spectra from irradiated samples are concerned, no modifications to the P3HT ^{1}H-NMR spectrum were observed even after 100 h of exposure (Fig. 1b). The reason for that might be the fact that also in this case the analysis is carried out on polymer solution, thus insoluble moieties formed during irradiation are excluded from the analysis.

Calorimetric measurements were carried out through DSC on all polymer samples in order to monitor the thermal transitions following irradiation. According to what reported in the literature [24], an endothermic transition was observed from a crystalline to a liquid crystalline state at a temperature of 220–240 °C (peak maximum 237 °C) for the pristine polymer. By means of calorimetric experiments, changes in the degree of crystallinity $X = \Delta H/\Delta H^0$ at increasing exposure times were also monitored, where ΔH is the actual enthalpy of fusion of the polymer and ΔH^0 is the enthalpy of fusion of the ideal crystal, taken as 99 J/g [25]. As it can be seen from Table 1, a very small variation in the degree of crystallinity of the polymer can be observed at increasing irradiation times.

The solid-state UV–Vis absorption spectrum of the pristine P3HT is shown in Fig. 2, where also the spectrum of 24 h irradiated P3HT is reported. The pristine polymer shows a maximum peak at 520 nm and two shoulders at 550 and 600 nm, respectively. After irradiation, a progressive decrease of the absorption intensity of the polymer was observed associated to a blue shift of the absorption band. These

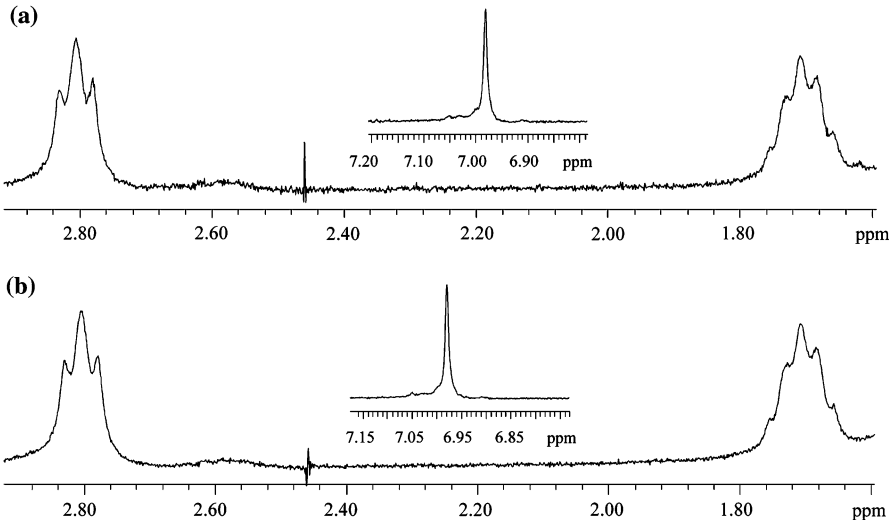

Fig. 1 Expanded ^{1}H-NMR spectra in the methylene region for pristine P3HT (**a**) and 100 h irradiated P3HT (**b**). Aromatic region is also shown in the *insets*

Table 1 Variation of degree of crystallinity of P3HT during exposure to simulated sunlight

Exposure time (h)	X (%)
0	21.4
48	19.8
96	19.9

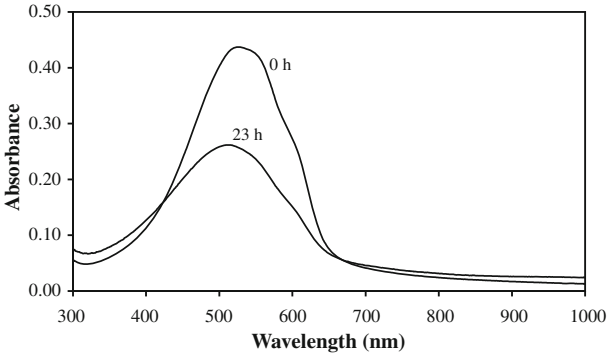

Fig. 2 UV–Vis absorption spectra of P3HT as a function of irradiation time (0 h, 24 h)

modifications can be attributed to the photobleaching of the polymer resulting from a reduction of the conjugation length. These observations are consistent with what reported in the literature [21] at longer exposure times.

Fourier-Transform infrared spectroscopy was used to monitor the kinetics of the photooxidation process. After irradiation, significant modifications of the IR spectra of the polymer were observed. In order to identify the changes occurring during irradiation, the main IR absorption bands for the pristine polymer have been identified and are reported in Table 2 [23].

A progressive decrease of absorption intensity was observed for various functional groups. In particular, the intensity of the absorption bands related to alkyl groups, aromatic C–H and thiophene ring rapidly decreased. As an example, Fig. 3 shows the progressive disappearance of the characteristic bands assigned to alkyl groups. As it can be noted, after approximately 50 h of exposure to simulated sunlight, the intensity of the peaks is decreased down to less than 50% of the original value.

In addition to the aforementioned trend, the simultaneous appearance of other absorption bands was reported. Several features appeared in the carbonyl region, as shown in Fig. 4, where different maxima can be distinguished upon irradiation. In the same graph, the disappearance of the band assigned to the thiophene ring stretching at 1,510 cm^{-1} (see Table 2) during exposure to simulated sunlight can be observed.

According to what reported above, Fig. 5 shows the time-dependent evolution of absorption intensity of different characteristic IR bands during irradiation. In order to make comparisons easier, normalized absorption intensities are reported.

Table 2 Frequencies and assignments of main IR bands for pristine P3HT

Wavenumber (cm^{-1})	Assignment
3,055	C–H (aromatic) str
2,955	CH_3 asym str
2,925	CH_2 asym str
2,855	CH_2 sym str
1,510 1,454	Thiophene ring str
820	C–H bend thiophene ring

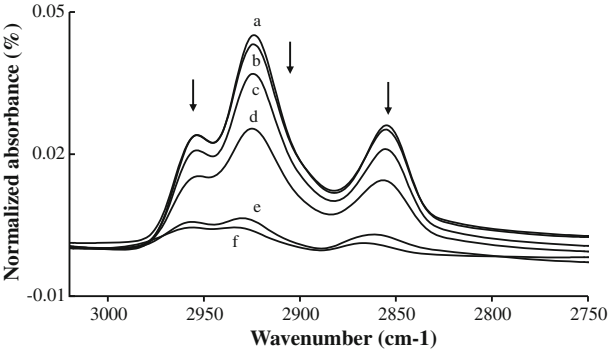

Fig. 3 Variation of FTIR spectra of P3HT spin-coated films in the aliphatic region as a function of irradiation time (*a*: 0 h; *b*: 6 h; *c*: 24 h; *d*: 48 h; *e*: 72 h; *f*: 100 h)

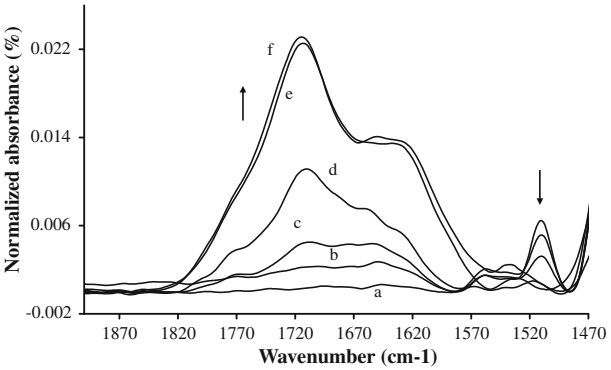

Fig. 4 Variation of FTIR spectra of P3HT spin-coated films in the carbonyl region as a function of irradiation time (*a*: 0 h; *b*: 6 h; *c*: 24 h; *d*: 48 h; *e*: 72 h; *f*: 100 h)

As shown in the graph, a decrease of intensity for signals attributed to alkyl groups and thiophene ring is observed accompanied by the appearance of new bands which may be assigned to carbonyl species and thioesters [21].

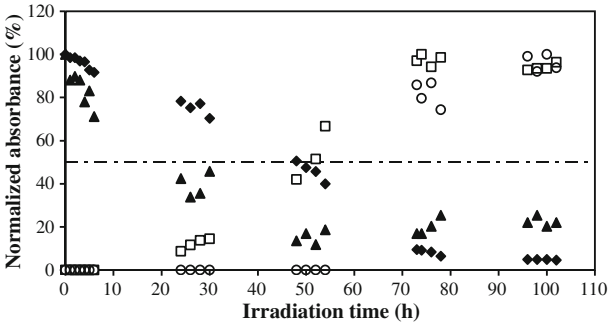

Fig. 5 Variation of normalized absorption intensity of characteristic groups in P3HT as a function of irradiation time: (*filled diamond*) alkyl groups in the range 3,000–2,800 cm^{-1}; (*filled triangle*) thiophene ring at 1,510 cm^{-1}; (*open square*) carbonyl groups at 1,715 cm^{-1}; (*open circle*) thioesters at 620 cm^{-1}

After about 50 h of exposure to simulated sunlight, the original absorption intensity is reduced by almost 50% for both alkyl groups and thiophene ring. At the same time, signals assigned to C=O stretching of carbonyl species and S=O stretching of thioesters progressively appear.

These trends may be attributed to modifications occurring to the macromolecular structure caused by a two-fold mechanism. On one side (Scheme 1), oxidations on the alkyl side-chain may occur resulting from the attack of oxygen to the carbon in α-position to the thiophene ring, which may lead to the formation of carbonyl species (1,715 cm^{-1}) since it is recognized that the carbon atom of a methylene in α-position to an unsaturated species is characterized by reduced C–H bond energy, thus representing a preferential site for radical attack [26].

On the other side (Scheme 2), modifications of the polymer backbone may occur leading to the opening of the thiophene ring. In particular bands assigned to thioesters (620 cm^{-1}), sulfoxides (1,050 cm^{-1}), dialkyl sulphones (1,150 cm^{-1}) and sulphones (1,190 cm^{-1}) were detected in the IR spectra of irradiated samples.

Considering what found so far, P3HT seems to show a remarkable instability towards photo-oxidation under simulated sunlight. In order to reduce the degradation rate of the polymer, potential stabilizing additives were therefore employed in this work. In particular two substances were chosen, one belonging to the class of Hindered Amine Light Stabilizers (HALS) and the other being Multi-Walled Carbon Nanotubes (MWCNT). The former was chosen because of its known ability to act as a radical scavenger in plastics and coatings technology. The latter was selected because it may act both as a radical scavenger [20] and quencher of excited

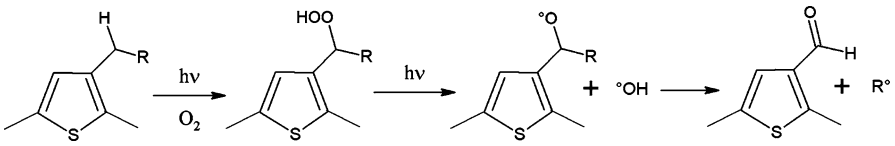

Scheme 1 Mechanism of photo-oxidation of lateral alkyl chain in P3HT

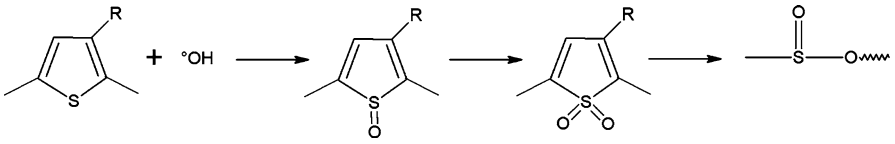

Scheme 2 Mechanism of photo-oxidation of polymer backbone in P3HT

states, and moreover it can be an efficient electron-acceptor photovoltaic component.

The HALS (5 wt%) was added to a solution of P3HT in chloroform (20 mg/mL), dissolved by magnetic stirring and then spin coated onto NaCl, KBr and CaF_2 substrates for FTIR analysis.

As far as the MWCNT system is concerned, a homogeneous dispersion of MWCNT in chloroform was prepared by ultrasonication for 90 min. The desired volume of the MWCNT dispersion was then added to a P3HT solution in chloroform (20 mg/mL) and a further 60 min ultrasonication was performed. The final concentration of the P3HT-MWCNT dispersion (20 mg/mL P3HT in chloroform—1 wt% MWCNT) was prepared by distillation of chloroform under vacuum and magnetic stirring. The dispersion was eventually spin coated onto NaCl, KBr and CaF_2 substrates for FTIR analysis.

The stabilizing effects of the two additives were monitored by means of FTIR. Figure 6 shows the changes of normalized absorption intensity of IR bands in the alkyl group region as a function of irradiation time The trend of neat P3HT is also reported, for reference.

No significant effects on the degradation rate of P3HT were reported after the addition of HALS to P3HT. On the other hand, a clear reduction in the degradation rate was observed when MWCNT were added. In particular, after about 100 h of exposure to simulated sunlight, a decrease of only 50% with respect to the original absorption intensity is observed in the case of P3HT-MWCNT blends. The same absorption intensity is reached after only 50 h of irradiation for neat P3HT and P3HT-HALS system.

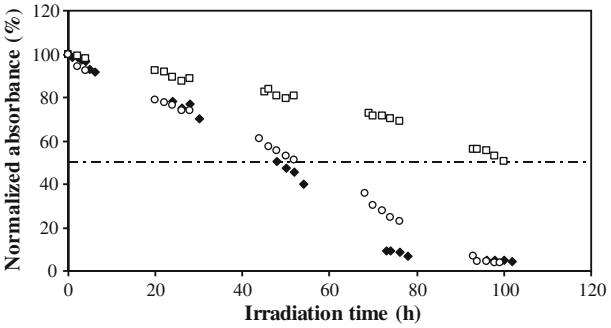

Fig. 6 Variation of normalized absorption intensity of the alkyl group IR signals as a function of irradiation time: (*filled diamond*) pure P3HT; (*open circle*) P3HT-HALS system; (*open square*) P3HT-MWCNT system

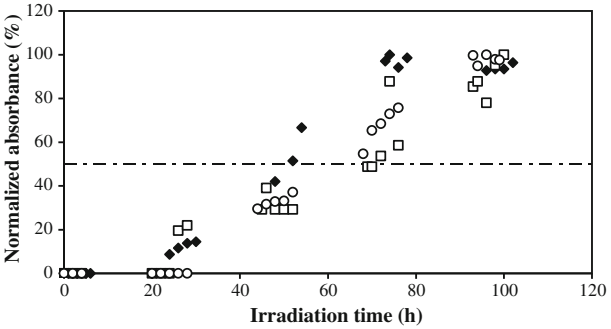

Fig. 7 Variation of normalized absorption intensity of IR signals related to carbonyl group as a function of irradiation time: (*filled diamond*) pure P3HT; (*open circle*) P3HT-HALS system; (*open square*) P3HT-MWCNT system

The time-dependent variation of normalized absorption intensity of IR bands related to carbonyl groups (1,715 cm^{-1}) during irradiation is reported in Fig. 7.

In this case both the presence of HALS and MWCNT appear to slightly slow down the degradation rate of P3HT. Moreover, the formation of carbonyl species appears to be slower for the P3HT-MWCNT system than for the P3HT-HALS one, according to the trend reported in Fig. 6. Similar trends were observed for the disappearance of IR signal assigned to the thiophene ring (1,510 cm^{-1}) and for the formation of the band assigned to thioesters (620 cm^{-1}).

The stabilizing effect of carbon nanotubes observed through FTIR in the P3HT-MWCNT blend might be explained by the radical scavenging properties of MWCNT which allow for a reduction of the degradation rate of P3HT. Similar results were actually observed on another system, namely poly[2-methoxy-5-(3′,7′-dimethyloctyloxy)-1,4-phenylenevinylene] (MDMO-PPV) blended with methano-fullerene [6,6]-phenyl C61-butyric acid methyl ester ([60] PCBM), suggesting that also PCBM can act as radical scavenger when mixed with P3HT and exposed to light [20].

The reduced stabilizing effect reported in the P3HT-HALS system could be attributed to the induction time needed by HALS molecules to activate and act as photo-stabilizers. Clearly, this induction time appears to be longer than the degradation rate of the neat polymer.

Conclusions

The results obtained from this work underline a substantial instability of P3HT to photooxidation following exposure to simulated sunlight. Modifications of the chemical structure of the polymer are observed, which corroborate the hypothesis of a degradation mechanism involving side-chain scission with formation of carbonyl species and aperture of the thiophene ring with formation of thioesters [11].

As a way to reduce photo-degradation rate, two substances were added to P3HT, namely a HALS and MWCNT, and the photo-chemical behaviour of these two new blends was investigated through FTIR.

While no significant effects were observed in the P3HT-HALS system, the addition of MWCNT to P3HT appeared to reduce significantly the degradation kinetics of the polymer, due to a radical scavenging effect of MWCNT. As a result, MWCNT might represent a good electron-acceptor candidate to improve photostability of organic solar cells.

References

1. Po R, Maggini M, Campioni N (2010) Polymer solar cells: recent approaches and achievements. J Phys Chem C 114:695–706
2. Jørgensen M, Norrman K, Krebs FC (2008) Stability/degradation of polymer solar cells. Sol Energy Mater Sol Cells 92:686–714
3. Krebs FC, Gevorgyan SA, Alstrup J (2009) A roll-to-roll process to flexible polymer solar cells: model studies, manufacture and operational stability studies. J Mater Chem 19:5442–5451
4. Krebs FC, Tromholt T, Jørgensen M (2010) Upscaling of polymer solar cell fabrication using full roll-to-roll processing. Nanoscale 1. doi:10.1039/b9nr00430k
5. Krebs FC (2009) All solution roll-to-roll processed polymer solar cells free from indium-tin-oxide and vacuum coating steps. Org Electron 10:761–768
6. Krebs FC, Norrman K (2010) Using light-induced thermocleavage in a roll-to-roll process for polymer solar cells. ACS Appl Mater Interfaces 2:877–887
7. Krebs FC, Gevorgyan SA, Gholamkhass B, Holdcroft S, Schlenker C, Thompson ME, Thompson BC, Olson D, Ginley DS, Shaheen SE, Alshareef HN, Murphy JW, Youngblood WJ, Heston NC, Reynolds JR, Jia S, Laird D, Tuladhar SM, Dane JGA, Atienzar P, Nelson J, Kroon JM, Wienk MM, Janssen RAJ, Tvingstedt K, Zhang F, Andersson M, Inganäs O, Lira-Cantu M, de Bettignies R, Guillerez S, Aernouts T, Cheyns D, Lutsen L, Zimmermann B, Würfel U, Niggemann M, Schleiermacher HF, Liska P, Grätzel M, Lianos P, Katz EA, Lohwasser W, Jannon B (2009) A round robin study of flexible large-area roll-to-roll processed polymer solar cell modules. Sol Energy Mater Sol Cells 93:1968–1977
8. Krebs FC, Jørgensen M, Norrman K, Hagemann O, Alstrup J, Nielsen TD, Fyenbo J, Larsen K, Kristensen J (2009) A complete process for production of flexible large area polymer solar cells entirely using screen printing—first public demonstration. Sol Energy Mater Sol Cells 93:422–441
9. Krebs FC, Nielsen TD, Fyenbo J, Wadstrøm M, Pedersen MS (2010) Manufacture, integration and demonstration of polymer solar cells in a lamp for the "Lighting Africa" initiative. Energy Environ Sci 3:512–525
10. Park SH, Roy A, Beaupré S, Cho S, Coates N, Moon JS, Moses D, Leclerc M, Lee K, Heeger AJ (2009) Bulk heterojunction solar cells with internal quantum efficiency approaching 100%. Nat Photonics 3:297–303
11. Roncali J (1992) Conjugated poly(thiophenes): synthesis, functionalization, and applications. Chem Rev 92:711–738
12. Norrman K, Gevorgyan SA, Krebs FC (2009) Water-induced degradation of polymer solar cells studied by $H_2^{18}O$ labeling. ACS Appl Mater Interfaces 1:102–112
13. Petersen MH, Gevorgyan SA, Krebs FC (2008) Thermocleavable low band gap polymers and solar cells therefrom with remarkable stability toward oxygen. Macromolecules 41:8986–8994
14. Krebs FC (2008) Air stable polymer photovoltaics based on a process free from vacuum steps and fullerenes. Sol Energy Mater Sol Cells 92:715–726
15. Abdou MSA, Holdcroft S (1993) Mechanisms of photodegradation of poly(3-alkylthiophenes) in solution. Macromolecules 26:2954–2962
16. Abdou MSA, Holdcroft S (1995) Solid-state photochemistry of π-conjugated poly(3-alkylthiophenes). Can J Chem 73:1893–1901
17. Ljungqvist N, Hjertberg T (1995) Oxidative degradation of poly(3-octylthiophene). Macromolecules 28:5993–5999
18. Caronna T, Forte M, Catellani M, Meille SV (1997) Photodegradation and photostabilization studies of poly(3-butylthiophene) in the solid state. Chem Mater 9:991–995

19. Chambon S, Rivaton A, Gardette JL, Firon M, Lutsen L (2006) Aging of a donor conjugated polymer: photochemical studies of the degradation of poly[2-methoxy-5-(3′,7′-dimethyloctyloxy)-1,4-phenylenevinylene]. J Polym Sci A Polym Chem 45:317–331
20. Chambon S, Rivaton A, Gardette JL, Firon M (2007) Photo- and thermal degradation of MDMO-PPV:PCBM blends. Sol Energy Mater Sol Cells 91:394–398
21. Manceau M, Rivaton A, Gardette JL, Guillerez S, Lemaître N (2009) The mechanism of photo- and thermooxidation of poly(3-hexylthiophene) (P3HT) reconsidered. Polym Degrad Stab 94:898–907
22. Manceau M, Rivaton A, Gardette JL (2008) Involvement of singlet oxygen in the solid-state photochemistry of P3HT. Macromol Rapid Commun 29:1823–1827
23. Chen TA, Wu X, Rieke RD (1995) Regiocontrolled synthesis of poly(3-alkylthiophenes) mediated by Rieke zinc: their characterization and solid-state properties. J Am Chem Soc 117:233–244
24. Hugger S, Thomann R, Heinzel T, Thurn-Albrecht T (2004) Semicrystalline morphology in thin films of poly(3-hexylthiophene). Colloid Polym Sci 282:932–938
25. Malik S, Nandi AK (2002) Crystallization mechanism of regioregular poly(3-alkyl thiophene)s. J Polym Sci B Polym Phys 40:2073–2085
26. Berkowitz J, Ellison GB, Gutman D (1994) Three methods to measure RH bond energies. J Phys Chem 98:2744–2765